Eddy Resolving Global Ocean Prediction including Tides

Alan J. Wallcraft
NRL Code 7323
Stennis Space Center, MS 39529-5004
phone: (228) 688-4813 fax: (228) 688-4759 email: Alan.Wallcraft@nrlssc.navy.mil

Award Number: N0001409WX20491
http://www.hycom.org, http://www7320.nrlssc.navy.mil/GLBhycom1-12/skill.html,
http://www7320.nrlssc.navy.mil/hycomARC

LONG-TERM GOALS

Use the HYbrid Coordinate Ocean Model (HYCOM) with tides, dynamic sea ice, and data assimilation in an eddy-resolving, fully global ocean prediction system with 1/25° horizontal resolution that will run in real time at the Naval Oceanographic Office (NAVOCEANO) starting in FY13. The model will include shallow water and provide boundary conditions to finer resolution coastal models that may use HYCOM or a different model.

OBJECTIVES

To develop, evaluate, and investigate the dynamics of 1/25° global HYCOM (HYbrid Coordinate Ocean Model) with tides coupled to CICE (Los Alamos Community Ice CodE) with atmospheric forcing only, with data assimilation via NCODA (NRL Coupled Ocean Data Assimilation), and in forecast mode. Also to incorporate advances in dynamics and physics from the science community into the HYCOM established and maintained within the Navy.

APPROACH

Traditional ocean models use a single coordinate type to represent the vertical, but no single approach is optimal for the global ocean. Isopycnal (density tracking) layers are best in the deep stratified ocean, pressure levels (nearly fixed depths) provide high vertical resolution in the mixed layer, and σ-levels (terrain-following) are often the best choice in coastal regions. The generalized vertical coordinate in HYCOM allows a combination of all three types (and others), and it dynamically chooses the optimal distribution at every time step via the layered continuity equation. HYCOM use a C-grid, has scalable, portable computer codes that run efficiently on available DoD High Performance Computing (HPC) platforms, and has a data assimilation capability.

Global HYCOM with 1/12° horizontal resolution at the equator (~7 km at mid-latitudes) is the ocean model component of the Global Ocean Forecast System (GOFS) 3.0 which is currently running in real time and which has passed its OPTEST on the Cray XT5 at the Naval Oceanographic Office (NAVOCEANO). It provides nowcasts and forecasts of the three dimensional global ocean environment. See http://www7320.nrlssc.navy.mil/GLBhycom1-12/skill.html for movies, snapshots and comparisons to observations and http://www.hycom.org for model fields. The other major

Report Documentation Page

Form Approved
OMB No. 0704-0188

1. REPORT DATE **2012**	2. REPORT TYPE **N/A**	3. DATES COVERED **-**
4. TITLE AND SUBTITLE **Eddy Resolving Global Ocean Prediction including Tides**		5a. CONTRACT NUMBER
		5b. GRANT NUMBER
		5c. PROGRAM ELEMENT NUMBER
6. AUTHOR(S)		5d. PROJECT NUMBER
		5e. TASK NUMBER
		5f. WORK UNIT NUMBER
7. PERFORMING ORGANIZATION NAME(S) AND ADDRESS(ES) **NRL Code 7323 Stennis Space Center, MS 39529-5004**		8. PERFORMING ORGANIZATION REPORT NUMBER
9. SPONSORING/MONITORING AGENCY NAME(S) AND ADDRESS(ES)		10. SPONSOR/MONITOR'S ACRONYM(S)
		11. SPONSOR/MONITOR'S REPORT NUMBER(S)

12. DISTRIBUTION/AVAILABILITY STATEMENT
Approved for public release, distribution unlimited

13. SUPPLEMENTARY NOTES
The original document contains color images.

14. ABSTRACT

15. SUBJECT TERMS

16. SECURITY CLASSIFICATION OF:			17. LIMITATION OF ABSTRACT	18. NUMBER OF PAGES	19a. NAME OF RESPONSIBLE PERSON
a. REPORT **unclassified**	b. ABSTRACT **unclassified**	c. THIS PAGE **unclassified**	**SAR**	**10**	

component of GOFS 3.0 is the NRL Coupled Ocean Data Assimilation (NCODA) which is a multivariate optimal interpolation scheme that assimilates surface observations from satellites, including altimeter and Multi-Channel Sea Surface Temperature (MCSST) data, sea ice concentration and also profile data such as XBTs (expendable bathythermographs), CTDs (conductivity temperature depth) and ARGO floats (Cummings, 2005). By combining these observations via data assimilation and using the dynamical interpolation skill of the model, the three dimensional ocean state can be accurately nowcast and forecast.

HYCOM has been coupled to the Los Alamos Community Ice CodE (CICE) (Hunke and Lipscomb, 2004) via the Earth System Modeling Framework (ESMF) (Hill et al., 2004). Coupling between the ocean and sea ice models more properly accounts for the momentum, heat and salt fluxes at the ocean/ice interface. GOFS 3.1, developed under this project, will include HYCOM coupled to CICE at 1/12° horizontal resolution and NCODA 3DVAR, rather than the MVOI used in GOFS 3.0.

The principal goal of this project is to perform the necessary R&D to prepare to provide a next-generation ocean nowcast/forecast system with real time depiction of the three-dimensional global ocean state at fine resolution (1/25° on the equator, 3.5 km at mid-latitudes, and 2 km in the Arctic). A major sub-goal of this effort is to test new capabilities in the existing 1/12° global HYCOM nowcast/forecast system and to transition some of these capabilities to NAVOCEANO in the 1/12° system, and others in the 1/25° global system. The new capabilities support (1) increased nowcast and forecast skill, the latter out to 30 days in many deep water regions, including regions of high Navy interest such as the Western Pacific and the Arabian Sea/Gulf of Oman, (2) boundary conditions for coastal models in very shallow, and (3) external and internal tides, the latter will initially be tested at 1/12°, to minimize computational cost, but will transition to NAVOCEANO only in the 1/25° system because at this resolution it will replace regional models with tides (all these will greatly benefit from the increase to 1/25° resolution). In addition to the NRL core tasking covered here, this effort will collaborate with a core team of similar size at FSU COAPS, with other parties interested in HYCOM development, and ONR field programs to test and validate the model in different regions and different regimes. Demonstrated advancements in HYCOM numerics and physics from all sources will be incorporated through this project.

WORK COMPLETED

The first 1/25º global HYCOM simulations (3.5 km resolution at mid-latitudes) were run three years ago with climatological 6-hourly atmospheric forcing. Two years ago we extended the simulation for 2003-2010 with 3-hourly NOGAPS atmospheric forcing, but still without data assimilation.

We ran the very first eddy resolving (1/12°) 3-D global ocean simulation with standard atmospheric forcing and tides in FY08 (Arbic et. al., 2010). Two years ago we performed a second multi-year simulation with an improved bottom tidal drag field, which was an exact twin of the 2003-2010 NOGAPS forced case mentioned above. Last year, and continuing this year, the results of these new simulations were extensively analyzed and were the subject of multiple papers.

Last year we made several improvements to how we handle tides: (a) a new bottom drag field based on bottom roughness from the 30" GEBCO_08 bathymetry, (b) a 48-hour filter on near-bottom currents, for tidal bottom drag, that stops all semi-diurnal tides but passes 70% of diurnal tides, and (c) a spatially varying “scalar” approximation to self-attraction and loading. In addition new 1/12° and

1/25° bathymetries were produced, also based on 30" GEBCO_08. With these improvements in hand, last year we started our 3rd global 1/12° simulation with NOGAPS and tides and the very first such global simulation at 1/25°. These were completed this year. In addition we have run a global 1/12° simulation with HYCOM coupled to the Los Alamos Community Ice CodE (CICE) via the Earth System Modeling Framework (ESMF) with NOGAPS and tides.

This year we have started running 1/25° global HYCOM with NCODA data assimilation. So far it has completed May 2010 to December 2011 and we expect to run it routinely every day in real time starting early in FY13.

The Arctic Cap Nowcast/Forecast System (ACNFS) consists of the subset of our tri-pole 1/12° global HYCOM domain that is north of 40°N (3.5 km resolution near the North Pole, 6.5 km at 40°N) coupled to CICE via tESMF with NCODA 3DVAR data assimilation of ocean state and sea ice concentration. It has run in hindcast mode from July 2007 and in real time since June 2010. It has passed its OPTEST on the IBM POWER6 at NAVOCEANO. For movies, snapshots and comparisons to the NIC frontal analysis, see http://www7320.nrlssc.navy.mil/hycomARC.

RESULTS

The FY12 ONR report by our collaborator Brain Arbic includes results from this past year obtained by Shriver and Richman at NRL under this project, and by Timko and Joseph Ansong, Arbic's postdocs. These results will not be repeated here. However, one additional aspect of Jim Richman's work on the wavenumber spectrum, why altimeter wavenumber spectra disagree with QG and SQG theory, is discussed below.

For QG and SQG turbulence, the shape of the spectra is determined by the energy and enstrophy cascades. QG theory assumes baroclinic energy is input into the ocean at large- and meso-scales and cascades towards the Rossby radius, where the baroclinic flow is transferred to the barotropic mode and an inverse cascade of energy to large scales occurs. Enstrophy cascades to small scales. For QG turbulence, while the KE and SSH spectra decrease steeply with wavenumber as k^{-3} and k^{-5}, respectively, the enstrophy spectrum is much flatter varying as k^{-1}. For SQG turbulence, the KE and SSH spectra decrease less steeply with wavenumber as $k^{-5/3}$ and $k^{-11/3}$, respectively, and the enstrophy spectrum increases slightly with wavenumber. The enstrophy spectra in the low EKE regions of the Pacific (Fig. 2b, d, and f) all exhibit relatively flat spectra falling between the expectation of the QG and SQG theory. The isotropic, geostrophic enstrophy spectral estimates obtained from the KE and SSH spectra are similar to the spectra obtained from the low passed vorticity. The isotropic estimates are small at low wavenumbers with a weak maximum before a steep decrease with increasing wavenumber. The isotropic enstrophy spectral peak shifts to short wavelengths with decreasing EKE.

The altimeter SSH wavenumber spectral slopes differ substantially from the model spectral slopes and the predictions of QG and SQG turbulence theory for most of the Pacific Ocean (Fig 1). There are a number of possible reasons for the differences. Internal waves have a flat wavenumber spectrum which when combined with the low-frequency SSH or velocity leads to a flattening of the spectral slopes over the fixed mesoscale band. The degree of flattening depends upon the relative strength of the high-frequency internal wave to QG motion. In addition, the difference between the model and altimeter spectral slope maps may be an artifact of the estimation over a fixed mesoscale band, which does not account for changes in the Rossby radius with latitude.

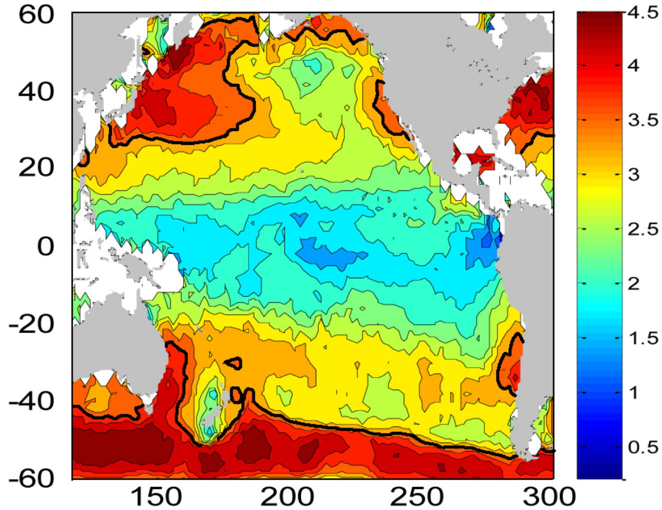

Figure 1. Slope of the along track satellite altimeter SSH wavenumber spectrum in the North Pacific for a 70-250 km band, adapted from (Xu and Fu, 2012). All slopes multiplied by -1 to make them positive. Slopes flatter than -11/3 (colors cooler than the enhanced dark contour) represent regions inconsistent with QG or SQG theory.

The model spectra decay rapidly with increasing wavenumber, while the altimeter spectra are flat at high wavenumber (black line in Figure 2c). The flat high wavenumber tail of the altimeter spectrum may represent the noise floor for the altimeter. Adding white noise equivalent to the altimeter noise floor to the model SSH yields a spectrum which is very similar to the observed altimeter SSH. In the high EKE regions, the energy in the mesoscale band is much greater than the noise floor and the spectral slope lies between the prediction of QG and SQG turbulence theory, while the noise flattens the spectral slope in lower EKE regions. Thus, the difference between the model and altimeter spectral slope estimates may have both dynamical causes due to internal waves and the characteristics of the energy and enstrophy cascades as well as instrumental causes.

When the wavenumber spectra of SSH and KE are estimated near the generating regions of internal tides, the resulting spectra are much flatter than the expectations of QG or SQG theory. This shows that in locations of energetic internal tides, the slope of the SSH or KE wavenumber spectrum in the mesoscale band cannot be used to infer the ocean dynamics unless the internal tides are accurately removed. For the HYCOM simulations with embedded tides, we can use the frequent (one-hour) sampling to separate high- and low-frequency motions more cleanly than is possible in altimeter data. If the height and velocity variability are separated into low frequency (periods greater than 36 hours) and high frequency (periods less than a day), then a different pattern emerges with a flat wavenumber spectrum at high frequency and a steeper wavenumber spectrum at low frequency. Away from generating regions where the internal waves are weaker than the QG flow, then the high frequency motions have little impact on the wavenumber spectrum. The global pattern of the slope of the mesoscale wavenumber spectrum, while showing regions of small, flatter slopes, does not agree quantitatively with the recent results of [5, 6] for the along track SSH wavenumber spectrum, which show very flat slopes away from regions of energetic eddies. Low passing the SSH and velocity yields spectra which lie between the expected slopes for Quasi-Geostrophic (QG) turbulence and Surface

Quasi-Geostrophic (SQG) turbulence. Even after removing the internal wave signal from the SSH and velocity, the spectral slopes can be flatter than either the QG or SQG predicted slope when estimated using a fixed mesoscale band. Altimeter noise affects the slope in the quieter mesoscale regions, which may explain differences between the model and altimeter spectra in some regions, for instance the tropics.

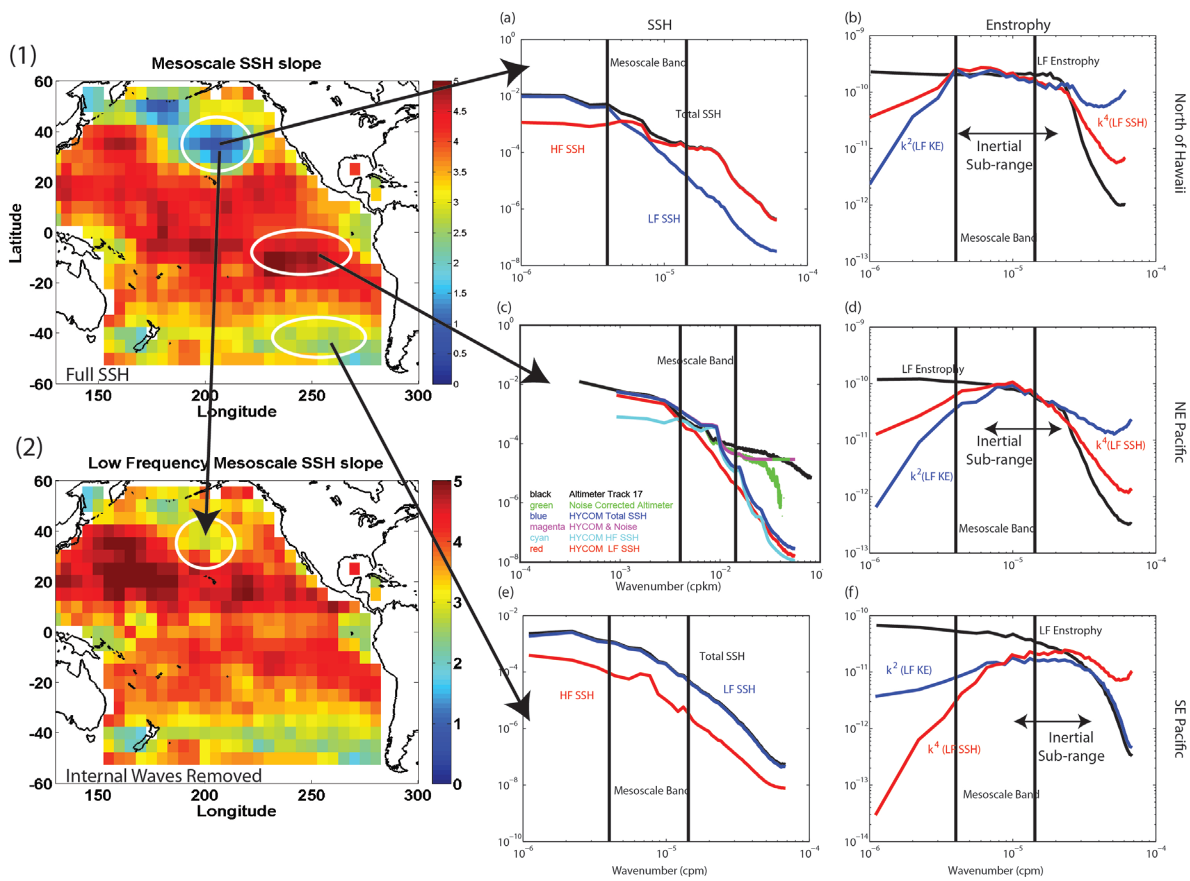

Figure 2. Maps of the least squares estimate of the slope of the HYCOM SSH wavenumber spectrum in the North Pacific, computed over a 70-250 km band. Slopes are computed from spectra of (1) total SSH and (2) low frequency SSH. Wavenumber spectra of sea surface height and enstrophy in three interior Pacific, lower EKE regions identified by the circles on the slope map, (a, b) Region north of Hawai'i (25°N, 210°E), (c, d) Northeast Pacific region (35°N, 230°E), and (e, f) Southeast Pacific region (35°S, 265°E). The spectra of total SSH (black), low frequency SSH (blue), and high frequency SSH (red) are shown in the left hand panels. The enstrophy spectra from the low frequency vorticity (black), the isotropic vorticity estimated from the low frequency kinetic energy (blue) and the isotropic vorticity estimated from the low frequency SSH (red) are shown in the right hand panels. Notice the shift in the enstrophy towards shorter wavelength as the EKE level decreases from top to bottom.

Experiments have begun to use the existing data assimilation scheme (NCODA, Cummings, 2005) with the new concurrent circulation and tide model. The results are encouraging as seen in Figure 3. In the upper left panel (Figure 3a), steric sea surface height (SSH) variance for a single day is shown for the model with tides. The hot spots of internal wave generations are clearly visible. In the upper right panel (Figure 3b), the steric SSH variance is shown for the model without tides, but assimilating data using the mesoscale covariances in NCODA applied to a daily averaged model background state. In this figure, high frequency variability is generated by baroclinic adjustment of the mesoscale eddies and meanders of strong ocean currents. The strength of the adjustment internal waves is similar to the strength of the internal tides, but the adjustment waves are strongest near the western boundary currents instead of the topographic hot spot generation sites. In the lower left panel (Figure 3c), the steric SSH variance for the model with tides and assimilation of mesoscale eddies via NCODA is shown. The SSH variance is larger than either the tide only model or assimilation only, with large variance at both the topographic hot spots and western boundary currents. In the lower right panel (Figure 3d), the difference in the SSH variance for the model with tides and assimilation and the sum of the variances from the tide only and data assimilation only models. The difference variance is lower than the variances of the individual models. The hot spots of tidal generation are not found in the difference plot suggesting that data assimilation of the mesoscale eddies is not affecting the tidal solution.

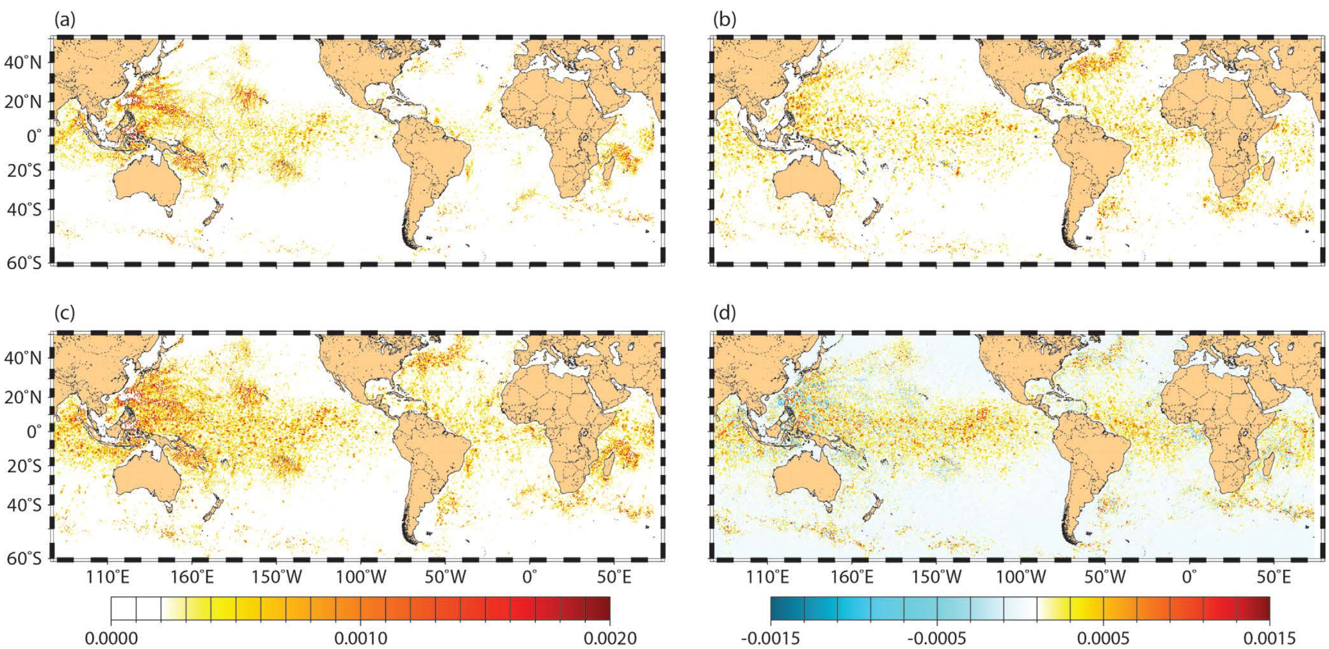

Figure 3. The steric sea surface variance for three model simulations, HYCOM with tides (a), HYCOM with data assimilation of mesoscale eddies using NCODA and HYCOM with tides and data assimilation (c). The lower left panel (d) shows the difference between HYCOM with tides and assimilation and the sum of the variances of HYCOM with tides only and HYCOM with assimilation only (c – (a+b)).

IMPACT/APPLICATIONS

The 1/25° (3.5 km mid-latitude) resolution is the highest so far for a global ocean model with high vertical resolution. A global ocean prediction system, based on 1/25° global HYCOM with tides, is planned to run in real-time starting in FY13 although initially without tides. At this resolution, a global ocean prediction system can directly provide boundary conditions to nested relocatable models with ~1 km resolution anywhere in the world, a goal for operational ocean prediction at NAVOCEANO. Internal tides and other internal waves can have a large impact on acoustic propagation and transmission loss (Chin-Bing et al., 2003, Warn-Varnas et al., 2003, 2007), which in turn significantly impacts Navy anti-submarine warfare and surveillance capabilities. At present, regional and coastal models often include tidal forcing but internal tides are not included in their open boundary conditions. By including tidal forcing and assimilation in a fully 3-D global ocean model we will provide an internal tide capability everywhere, and allow nested models to include internal tides at their open boundaries.

TRANSITIONS

Both the Global Ocean Forecast System (GOFS) 3.0 and the Arctic Cap Nowcast/Forecast System (ACNFS) have passed OPTEST at NAVOCEANO and will become operational on their new IBM iDataPlex systems once they are available early in FY13.

RELATED PROJECTS

There are two related ONR funded projects, one at FSU COAPS under Eric Chassignet and the other at U. Michigan under Brian Arbic. Partnering projects at NRL include 6.1 Ageostrophic Vorticity Dynamics of the Ocean and its Impact on Frontogenesis, 6.1 Determining the Impact of Sea Ice Thickness on the Arctic's Naturally Changing Environment (DISTANCE), 6.2 Full Column Mixing for Numerical Ocean Models, 6.3 Ocean Reanalysis, 6.4 Large Scale Ocean Modeling, 6.4 Ocean Data Assimilation, and 6.4 Ice Modeling Assimilation from Satellites. The computational effort is strongly supported by DoD HPC Challenge and NRL non-challenge grants of computer time. In FY12 some 1/25° and some 1/12° global HYCOM cases ran under a 6 months extension to a FY09-11 DoD HPC Challenge grant.

REFERENCES

Arbic, B.K., A.J. Wallcraft and E.J. Metzger, 2010: Concurrent simulation of the eddying general circulation and tides in a global ocean model. Ocean Modelling, 32, 175-187.

Chin-Bing, S.A., A. Warn-Varnas, D.B. King, K.G. Lamb, M. Teixeira, and J.A. Hawkins, 2003: Analysis of coupled oceanographic and acoustic soliton simulations in the Yellow Sea: a search for soliton-induced resonances. Mathematics and Computers in Simulation, 62, 11-20.

Cummings, J.A., 2005. Operational multivariate ocean data assimilation. *Quart. J. Royal Met. Soc.,* 131 (613), 3583-3604.

Ducet, N., P. -Y. Le Traon, and G. Reverdin (2000), Global high resolution mapping of ocean circulation from TOPEX/Poseidon and ERS-1 and 2, J. Geophys. Res., 105, 19477-19498.

Hill C., C. DeLuca, V. Balaji, M. Suarez, A. da Silva, 2004. The Architecture of the Earth System Modeling Framework. *Computing in Science and Engineering,* **6**, 18-28.

Hollinger, J.P., 1991. DMSP Special Sensor Microwave/Imager Calibration/Validation – Final Report Volume II", Naval Research Laboratory, Washington, DC.

Hunke, E.C. and W.H. Lipscomb, 2004. CICE: the Los Alamos sea ice model documentation and software user's manual. http://climate.lanl.gov/Models/CICE

Lebedev, K. V., H. Yoshinari, N. A. Maximenko, and P. W. Hacker (2007), Velocity data assessed from trajectories of Argo floats at parking level and at the sea surface, IPRC Technical Note No. 4(2), Honolulu, 16pp.

Markus, T. and D.J. Cavalieri, 2000. An Enhancement of the NASA Team Sea Ice Algorithm. *IEEE Trans Geoscience Remote Sensing*, vol. 38, pp. 1387-1398, 2000.

Scott, R. B., B. K. Arbic, E. P. Chassignet, A. C. Coward, M. Maltrud, W. J. Merryfield, A. Srinivasan, and A. Varghese (2010), Total kinetic energy in four global eddying ocean circulation models and over 5000 current meter records, Ocean Modell., 32, 157-169.

Warn-Varnas, A.C., S.A. Chin-Bing, D.B. King, Z. Hallock, and J.A. Hawkins, 2003. Ocean-acoustic solitary wave studies and predictions. Surveys in Geophysics, 24, 39-79.

Warn-Varnas, A.C., S.A. Chin-Bing, D.B. King, J.A. Hawkins, K.G. Lamb, and J.F. Lynch, 2007. Winter PRIMER ocean-acoustic solitary wave modeling studies. IEEE J. Oceanic Engineering, 32(2), 436-452.

Xu, Y., and L.L. Fu (2012), The effects of altimeter instrument noise on the estimation of the wavenumber spectrum of sea surface height. J. Phys. Oceanogr., doi:10.1175/JPO-D-12-0106.1, in press.

PUBLICATIONS

Arbic, B.K., J.G. Richman, J.F. Shriver, P.G. Timko, E.J. Metzger and A.J. Wallcraft, 2012: Global Modeling of Internal Tides Within an Eddying Ocean General Circulation Model. *Oceanography*, **25**, 20-29 doi:http://dx.doi.org/10.5670/oceanog.2012.38. [published, refereed]

González-Rodríguez, E., Trasviña-Castro, A., Gaxiola-Castro, G., Zamudio, L., and R. Cervantes-Duarte, 2012: Net primary productivity, upwelling and coastal currents in the Gulf of Ulloa, Baja California, Mexico, *Ocean Sci.*, **8**, 703–711, 2012, www.ocean-sci.net/8/703/2012/, doi:10.5194/os-8-703-2012. [published, refereed]

Hebert, D.A., J.A. Cummings, P.G. Posey, R. H. Preller, A.J. Wallcraft, M.W. Phelps, O.M. Smedstad and R. Wilkins, 2012: Forecasting Arctic Conditions with the Arctic Cap Nowcast/Forecast System, *Journal of Atmospheric and Oceanic Technology* [refereed]

Jia, Y., P.H.R. Calil, E.P. Chassignet, E.J. Metzger, J.T. Potemra, K.J. Richards, and A.J. Wallcraft 2011: Generation of mesoscale eddies in the lee of the Hawaiian Islands. *J. Geophys. Res.*, **116**, C11009, doi:10.1029/2011JC007305. [published, refereed]

Joseph, S., A.J. Wallcraft, T.G. Jensen, M. Ravichandran, S.S.C. Shenoi and S.Nayak, 2012: Weakening of spring Wyrtki jets in the Indian Ocean during 2006-2011. *J. Geophys. Res.*, **117**, C04012, doi:10.1029/2011JC007581. [published, refereed]

Metzger, E.J., O.M. Smedstad, P.G. Thoppil, J.A. Cummings, P.J. Hogan, H.E. Hurlburt, A.J. Wallcraft, and D.S. Franklin, 2012: A Global Ocean Nowcast/Forecast System Based on the 0.08° HYbrid Coordinate Ocean Model and the Navy Coupled Ocen Data Assimilation System. *J. Marine Sci.* [refereed]

Posey, P.G., E.J. Metzger, R.A. Allard, R.H. Preller, D. Hebert, A.J. Wallcraft, M.W. Phelps, J. Hutchings, O.M. Smedstad and R. Wilkins, 2012: Arctic Cap Nowcast/Forecast System (ACNFS) End of Summer 2012 Ice Extent Projection. Sea Ice Outlook Project website, July 2012. [published]

Posey, P.G., E.J. Metzger, R.A. Allard, R.H. Preller, D. Hebert, A.J. Wallcraft, M.W. Phelps, J. Hutchings, O.M. Smedstad and R. Wilkins, 2012: Arctic Cap Nowcast/Forecast System (ACNFS) End of Summer 2012 Ice Extent Projection. Sea Ice Outlook Project website, August 2012. [published]

Posey, P.G., E.J. Metzger, R.A. Allard, R.H. Preller, D. Hebert, A.J. Wallcraft, M.W. Phelps, J. Hutchings, O.M. Smedstad and R. Wilkins, 2012: Arctic Cap Nowcast/Forecast System (ACNFS) End of Summer 2012 Ice Extent Projection. Sea Ice Outlook Project website, September 2012. [published]

Richman, J.G., B.K. Arbic, J.F. Shriver, E.J. Metzger and A.J. Wallcraft, 2012: Inferring Dynamics from the Wavenumber Spectra of an Eddying Global Ocean Model with Embedded Tides. *J. Geophys. Res.* [refereed]

Richman, J.G., E.J. Metzger, J.F. Shriver, A.J. Wallcraft, O.M. Smedstad and B.K. Arbic, 2012: Predicting tides in a high resolution ocean general circulation model. HPCMP DOD Mission Success Book.

Richman, J.G., J.F. Shriver, and B.K. Arbic, 2012: Can we infer ocean dynamics from wavenumber spectrum? Proceedings of the "20 Years of Progress in Radar Altimetry" Symposium, 24-29 Sept 2012, Venice, Italy.

Richman, J.G., J.F. Shriver, E.J. Metzger, P.J. Hogan, G.A. Jacobs and B.K.Arbic, 2012: Oceanic hot spots – internal tides in the global ocean. 2012 NRL Review.

Richman, J.G., P.G. Thoppil, P.J. Hogan, and A.J. Wallcraft 2011: What is required to model the global ocean circulation? Proceedings of the 2011 HPCMP User's Group Conference, Portland, OR. [published]

Shinoda, T., W. Han, E. J. Metzger and H. E. Hurlburt, 2012: Seasonal Variation of the Indonesian Throughflow in Makassar Strait. *Journal of Physical Oceanography*, **42**, 1099-1123, doi:10.1175/JPO-D-11-0120.1. [published, refereed]

Shriver, J.F., B.K. Arbic, J.G. Richman, R.D. Ray, E.J. Metzger, A.J. Wallcraft and P.G. Timko, 2012: An Evaluation of the Barotropic and Internal Tides in a High Resolution Global Ocean Circulation Model. *J. Geophys. Res.* [in press, refereed]

Shriver, J.F., J.G. Richman, B.K. Arbic, R.D. Ray, E.J. Metzger and A.J. Wallcraft, 2012: How stationary are the internal tides in a high resolution global ocean circulation model? Proceedings of the "20 Years of Progress in Radar Altimetry" Symposium, 24-29 Sept 2012, Venice, Italy.

Timko, P.G., B.K. Arbic, J.G. Richman, R.B. Scott, E.J. Metzger and A.J. Wallcraft, 2012: Skill tests of three-dimensional tidal currents in a global ocean model: A look at the North Atlantic. J. *Geophys. Res.*, **117**, C08014 doi:10.1029/2011JC007617. [published, refereed]

Timko, P.G., B.K. Arbic, J.A. Goff, W.H.F. Smith, and A.J. Wallcraft, 2012: The effect of Synthetic Abyssal Hill Roughness on Internal Tide Generation in Global Numerical Models. *J. Geophys. Res.* [refereed]

Trasviña, A., K. J. Heywood, A. H. H. Renner, S.E. Thorpe, A. F. Thompson, and L. Zamudio (2011), The impact of high frequency currents on dispersion off the eastern Antarctic Peninsula. *J. Geophys. Res.*, **116**, C11024, doi:10.1029/2011JC007003. [published, refereed]

Trossman, D.S., B.K. Arbic, S.T. Garner, J.A. Goff, S.R. Jayne, E.J. Metzger, and A.J. Wallcraft, 2012: Impact of Topographic Internal Wave Drag on the Energy Budget of a High-Resolution Global Ocean General Circulation Model. *J. Geophys. Res.* [refereed]